# A COMPARATIVE STUDY OF
# RAYLEIGH FADING WIRELESS CHANNEL SIMULATORS

A Thesis

by

VISHNU RAGHAVAN SATHINI RAMASWAMY

Submitted to the Office of Graduate Studies of
Texas A&M University
in partial fulfillment of the requirements for the degree of

MASTER OF SCIENCE

December 2005

Major Subject: Electrical Engineering

# A COMPARATIVE STUDY OF
# RAYLEIGH FADING WIRELESS CHANNEL SIMULATORS

A Thesis

by

VISHNU RAGHAVAN SATHINI RAMASWAMY

Submitted to the Office of Graduate Studies of
Texas A&M University
in partial fulfillment of the requirements for the degree of

MASTER OF SCIENCE

Approved by:

| | |
|---|---|
| Chair of Committee, | Scott Miller |
| Committee Members, | Costas Georghiades |
| | Shankar Bhattacharyya |
| | Daren Cline |
| Head of Department, | Costas Georghiades |

December 2005

Major Subject: Electrical Engineering

# ABSTRACT

A Comparative Study of

Rayleigh Fading Wireless Channel Simulators. (December 2005)

Vishnu Raghavan Sathini Ramaswamy, B.E, Birla Institute of Technology and Science, Pilani

Chair of Advisory Committee: Dr. Scott Miller

Computer simulation is now increasingly being used for design and performance evaluation of communication systems. When simulating a mobile wireless channel for communication systems, it is usually assumed that the fading process is a random variate with Rayleigh distribution. The random variates of the fading process should also have other properties, like autocorrelation, spectrum, etc. At present, there are a number of methods to generate the Rayleigh fading process, some of them quite recently proposed. Due to the use of different Rayleigh fading generators, different simulations of the same communication system yield different results. Three methods, viz., the Jakes method, the IDFT method and the filtering WGN method, have been studied, simulated and compared based on the Rayleigh fading process' properties. Various communication systems have been simulated using the Rayleigh fading generators and the difference in the results, if any, have been analyzed. The research studies the different Rayleigh fading generators and compares them using the properties of the Rayleigh fading channel. It is found that the IDFT method and the filtering WGN method generate processes that have properties very close to the ideal Rayleigh fading process.

To my parents

# ACKNOWLEDGMENTS

I would like to thank my advisor Dr. Scott Miller for his invaluable guidance, support and advice without which this thesis would not have been possible. I thank my Committee members Dr. Costas Georghiades, Dr. Shankar Bhattacharyya and Dr. Daren B.H. Cline for their time and consideration. I thank Dr. Krishnan Narayanan for his support. I thank the Electrical Engineering Department, TexasA&M University for providing the infrastructure for the research. I would like to thank my friends Gopi, Kota and Siva for their help.

TABLE OF CONTENTS

CHAPTER Page

I INTRODUCTION . . . . . 1

II BACKGROUND ON LAND MOBILE FADING CHANNELS . 3

A. Multipath Rayleigh fading . . . . . 3
B. Properties of Rayleigh fading process . . . . . 7
1. Autocorrelation function and power spectral density . 7
2. Level crossing rate and fade duration . . . . . 10

III RAYLEIGH FADING PROCESS GENERATION METHODS . 12

A. Sum of sinusoids or Jakes method . . . . . 12
B. IDFT method . . . . . 14
C. Filtering white Gaussian noise . . . . . 18

IV COMPARISON OF RAYLEIGH FADING PROCESS GENERATORS . . . . . 24

A. Comparison of characteristics of the generated processes . 25
1. Rayleigh distribution . . . . . 25
2. Autocorrelation function . . . . . 28
3. Fade duration and level crossing rate . . . . . 39
4. Computational complexity . . . . . 40

V CONCLUSION . . . . . 43

REFERENCES . . . . . 45

VITA . . . . . 47

# LIST OF TABLES

TABLE Page

I Level crossing rate and fade duration of the Rayleigh fading processes got from different generators and normalized to the expected values . . . . . 40

II Time required to generate 200,000 points of Rayleigh distributed variables using different generation methods . . . . . 42

# LIST OF FIGURES


| FIGURE | | Page |
|---|---|---|
| 1 | Scattering environment in a typical macrocell | 4 |
| 2 | Rayleigh fading channel model | 5 |
| 3 | Rayleigh fading envelope | 6 |
| 4 | Autocorrelation function of Rayleigh fading process | 9 |
| 5 | Power spectrum of Rayleigh fading process | 10 |
| 6 | Jakes' model | 13 |
| 7 | Magnitude response of second and third order filters | 19 |
| 8 | The autocorrelation function produced by filters of different orders | 20 |
| 9 | Cumulative distribution of fading coefficients generated by different methods | 26 |
| 10 | Difference in cumulative distribution of fading coefficients generated by different methods and the expected Rayleigh distribution | 27 |
| 11 | BER curves for BPSK modulation in Rayleigh fading environment and AWGN using the IDFT method and filtering WGN method | 28 |
| 12 | BER curves for BPSK modulation in Rayleigh fading environment and AWGN using the two Jakes methods | 29 |
| 13 | Difference between simulated BER and expected BER for BPSK modulation in Rayleigh fading environment and AWGN using different Rayleigh fading generators | 30 |
| 14 | BER curves for 16-PSK modulation in Rayleigh fading environment and AWGN using different Rayleigh fading generators | 31 |

FIGURE Page

15 BER curves for 16-QAM modulation in Rayleigh fading environment and AWGN using different Rayleigh fading generators . . . . . 31

16 Block diagram of the simulated transmitter . . . . . 32

17 Block diagram of the simulated receiver . . . . . 32

18 Autocorrelation of the processes produced by the Jakes methods . . . 33

19 Autocorrelation of the processes produced by the IDFT method and filtering WGN method . . . . . 34

20 Simulated block error rates for BCH(127,50,13) code with 127*4 interleaving matrix . . . . . 35

21 Simulated block error rates for Golay code with 23*10 interleaving matrix . . . . . 36

22 Simulated block error rates for Golay code . . . . . 37

23 Autocorrelation function of the Rayleigh fading process generated by the 15th order AR filter . . . . . 38

24 Simulated block error rates for BCH(127,8,31) code . . . . . 38

# CHAPTER I

## INTRODUCTION

Simulation of wireless channels accurately is very important for the design and performance evaluation of wireless communication systems and components. When simulating the wireless channel for mobile and macro cellular communications, it is usually assumed that the fading process is a Rayleigh fading process. The discrete samples of the Rayleigh fading process have a Rayleigh distribution and are correlated. For generating the Rayleigh fading coefficients, three different methods of random variate generations are used.

The model proposed by Jakes [1] is a commonly accepted model of a multipath fading environment. The initial simulation method that was used and that is still widely used is the Sum of sinusoids method proposed by Jakes [1], [12]. The fading process can also be realized by passing complex Gaussian noise through an ARMA filter [9], [12] or by an algorithm based on inverse discrete Fourier transform [11], [14].

For the same application, i.e., for a particular channel coding technique, interleaving block size, Doppler shift, etc., it is found that simulations using the different algorithms yield different results. Despite the need of an accurate and an efficient method for generating the Rayleigh fading process, there is no sure method available in the literature to find the best generation method for simulating a given communication system.

This report attempts to find a well suited Rayleigh fading process generation technique given a communication system.

Chapter II explains multipath Rayleigh fading and deals with the properties

---

The journal model is *IEEE Transactions on Automatic Control.*

of Rayleigh fading. Chapter III explains the three main Rayleigh fading process generators and the intuitive ideas behind them.

Chapter IV compares the three generation methods based on the Rayleigh fading properties explained in Chapter II. Some communication systems are simulated using different generation methods and the difference in the simulation results are explained in relation to the fading properties. Chapter V concludes the work.

# CHAPTER II

## BACKGROUND ON LAND MOBILE FADING CHANNELS

### A. Multipath Rayleigh fading

In a wireless system, a signal transmitted into the channel interacts with the environment in a very complex way, bouncing off various surfaces along the way to the receiver. There are reflections from large objects, diffraction of electromagnetic waves around objects and signal scattering as shown in Figure 1. The result of these complex interactions is the presence of many signal components, or multipath signals, at the receiver. In addition to this, if the transmitter, receiver or the objects in the path of the signal are in motion, Doppler shift is introduced. As a result of these two phenomenon, the received signal is time varying and may be highly attenuated. This is a major impairment in a wireless communication system.

At any given time instance, a number of plane waves will be incident on the mobile antenna. Assume that the career frequency is $f_c$, and the mobile station is moving at a velocity of v. If the nth wave is incident on the mobile antenna at an angle of $\theta_n(T)$ relative to the direction of motion of the mobile, the Doppler shift introduced in the incident wave is given by

$$f_{D,n}(t) = f_d \cos\theta_n(t), \tag{2.1}$$

where $f_d = v/\lambda_c$ and $\lambda_c$ is the wavelength of the transmitted signal. If the transmitted signal s(t) is given by $Re\{u(t)e^{j2\pi f_c t}\}$ where u(t) is the complex lowpass signal, v(t), the received complex lowpass signal is given by

$$v(t) = \sum_{n=1}^{N} \alpha_n(t) e^{-j2\pi[(f_c + f_{D,n}(t))\tau_n(t) - f_{D,n}(t)t]} u(t - \tau_n(t)), \tag{2.2}$$

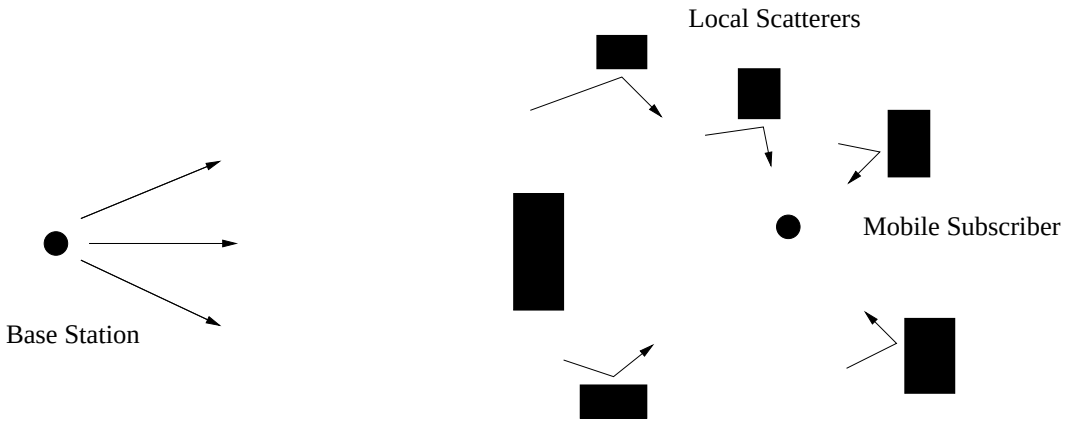


Fig. 1. Scattering environment in a typical macrocell

where N is the total number of incident waves and $\alpha_n(t)$ and $\tau_n(t)$ are the amplitude and time delay, respectively, associated with the nth path.

Equation 2.2 can be rewritten as

$$v(t) = \sum_{n=1}^{N} \alpha_n(t) e^{-j\phi_n(t)} u(t - \tau_n(t)) \tag{2.3}$$

and

$$\phi_n(t) = 2\pi\{(f_c + f_{D,n}(t))\tau_n(t) - f_{D,n}(t)t\} \tag{2.4}$$

is the phase associated with the nth wave. It can be seen that this multipath fading affects different frequency components of the transmitted signal differently. In fading, there is a parameter called coherence bandwidth which is a statistical measure of the range of frequencies over which the channel can be considered "flat". It can also be described as the range of frequencies over which two frequency components have a strong amplitude correlation. If $\tau_k$ is defined as the time delay of the kth multipath component and $\bar{\tau}$ is the mean delay spread, the rms delay spread is defined as

$$\sigma_\tau = \sqrt{\bar{\tau^2} - (\bar{\tau})^2} \tag{2.5}$$

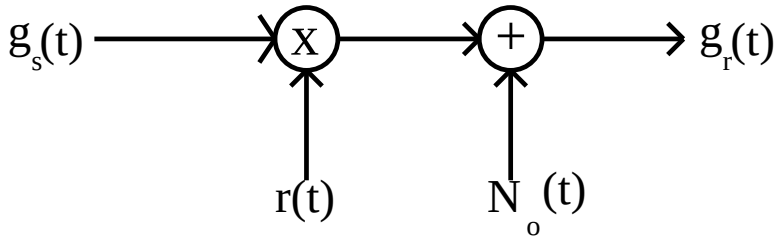


Fig. 2. Rayleigh fading channel model

If a mobile radio channel has a constant gain and linear phase response over a bandwidth (coherence bandwidth) which is greater than the bandwidth of the transmitted signal, the signal is said to undergo flat fading. It can be said that, a signal undergoes flat fading if its bandwidth is less than the channel's coherence bandwidth and its symbol duration is greater than the rms delay spread. This type of fading is the most common type of fading that is described in technical literature. This is the type of fading this report deals with. For flat fading channels, the fading can be modeled as a time variant multiplying factor r(t).

It is shown in [8] that the received signal in a multipath channel is modeled as

$$g_r(t) = r(t)g_s(t) + N_o(t), \tag{2.6}$$

where $g_s$ is the transmitted signal, $g_r$ is the received signal, $N_o(t)$ is the additive noise and r(t)=x(t)+jy(t) is the Rayleigh fading coefficient. The model is shown in Figure 2. Rayleigh distributed variates can be obtained as the magnitude of complex Gaussian distributed variates. An example of Rayleigh fading envelope is shown in Figure 3.

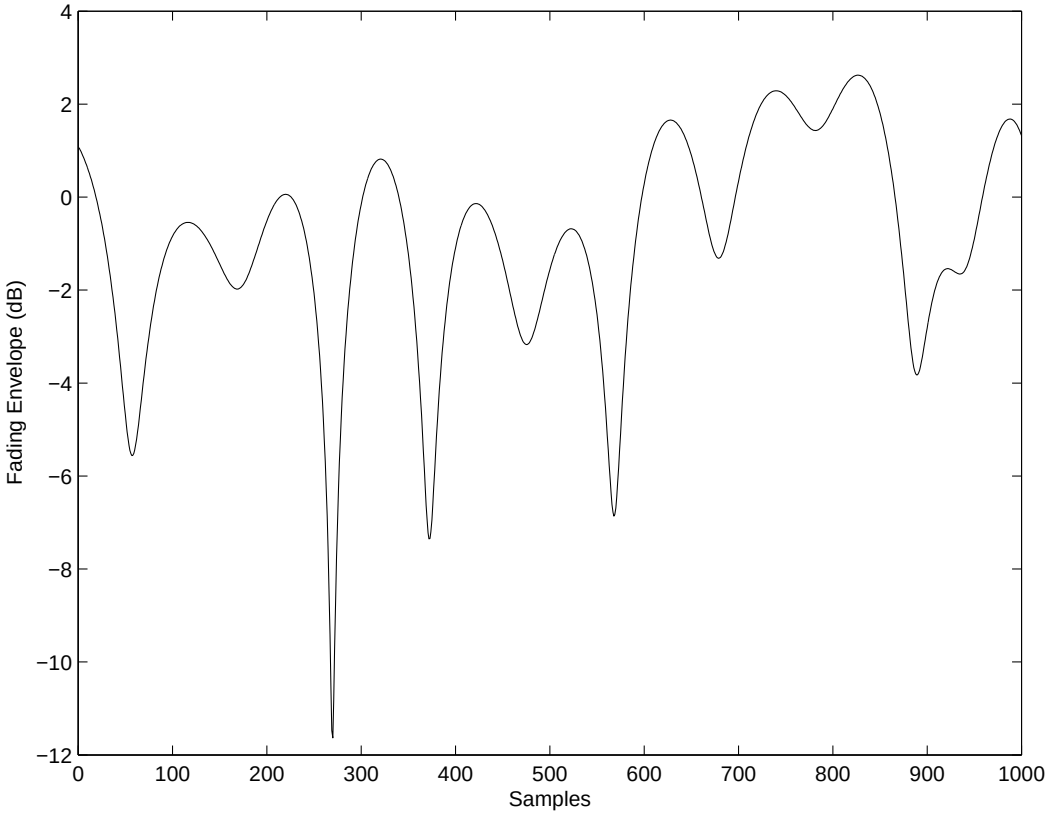


Fig. 3. Rayleigh fading envelope

## B. Properties of Rayleigh fading process

Since the fading effect on all the transmitted frequencies is assumed to be uniform, the properties of the Rayleigh fading process can be derived assuming the transmitted signal is an unmodulated carrier. For the unmodulated carrier, the received complex lowpass signal is

$$r(t) = \sum_{n=1}^{N} \alpha_n(t) e^{-j\phi_n(t)} \tag{2.7}$$

or

$$r(t) = r_I(t) + j r_Q(t), \tag{2.8}$$

where

$$r_I(t) = \sum_{n=1}^{N} \alpha_n(t) \cos \phi_n(t) \tag{2.9}$$

and

$$r_Q(t) = \sum_{n=1}^{N} \alpha_n(t) \sin \phi_n(t). \tag{2.10}$$

As N increases, the central limit theorem can be invoked and $r_I(t)$ and $r_Q(t)$ can be treated as independent Gaussian random processes with zero mean. This would make r(t) a complex random process whose real and imaginary components are independent Gaussian random processes. Thus the magnitude of r(t) is a Rayleigh distributed process. Hence the term Rayleigh fading envelope is applied to r(t). If there are fixed scatterers or a line of sight path for the radio waves, $r_I(t)$ and $r_Q(t)$ can no longer be modeled as having zero-mean. In such cases, the magnitude of r(t) has a Ricean distribution and such fading is called Ricean fading.

### 1. Autocorrelation function and power spectral density

Assuming that all the random processes involved are wide sense stationary, the autocorrelation function (ACF) $\phi_{r_I r_I}(\tau)$ can be calculated from equations 2.9, 2.1 and

2.4 as follows [12]:

$$\begin{aligned}\phi_{r_I r_I}(\tau) &= E[r_I(t) r_I(t+\tau)] \\ &= E[\cos 2\pi f_{D,n}\tau] \\ &= E_\theta[\cos(2\pi f_d \tau \cos\theta)]. \end{aligned} \tag{2.11}$$

Here it is assumed that

$$E[r_I^2(t)] = E[r_Q^2(t)] = \frac{1}{2}\sum_{n=1}^{N} E[\alpha_n^2] = 1 \tag{2.12}$$

i.e., the total average power received from all multipath components is one. Similarly, the cross correlation $\phi_{r_I r_Q(\tau)}$ can be calculated as

$$\begin{aligned}\phi_{r_I r_Q}(\tau) &= E[r_I(t) r_I(t+\tau)] \\ &= E_\theta[\sin(2\pi f_d \tau \cos\theta)]. \end{aligned} \tag{2.13}$$

For macro cellular environments, the MS antenna receives the plane waves from all directions with equal probability. So, it is reasonable to assume that $\theta$ is uniformly distributed over $[-\pi, \pi]$. This model is referred to as Clarke's two-dimensional isotropic scattering model. With this assumption, 2.11 becomes

$$\begin{aligned}\phi_{r_I r_I}(\tau) &= \frac{1}{2\pi}\int_{-\pi}^{\pi} \cos(2\pi f_d \tau \cos\theta) d\theta \\ &= \frac{1}{\pi}\int_{0}^{\pi} \cos(2\pi f_d \tau \sin\theta) d\theta \\ &= J_0(2\pi f_d \tau), \end{aligned} \tag{2.14}$$

where $J_0(x)$ is the zeroth-order Bessel function of the first kind. The autocorrelation function is displayed in Figure 4. Similarly, 2.13 becomes

$$\phi_{r_I r_Q}(\tau) = \frac{1}{2\pi}\int_{-\pi}^{\pi} \sin(2\pi f_d \tau \cos\theta) d\theta$$

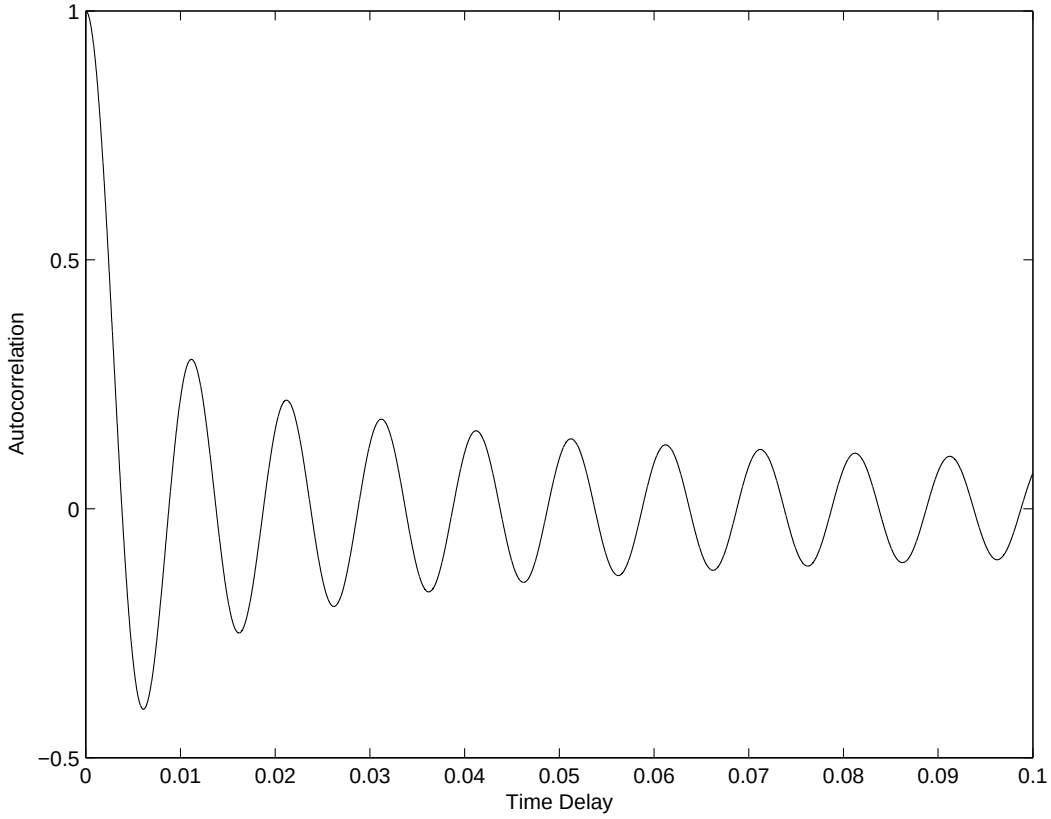


Fig. 4. Autocorrelation function of Rayleigh fading process

$$= \quad 0. \tag{2.15}$$

Also note that

$$\phi_{r_I r_I}(\tau) = \phi_{r_Q r_Q}(\tau) \tag{2.16}$$

and

$$\phi_{r_I r_Q}(\tau) = \phi_{r_Q r_I}(\tau). \tag{2.17}$$

The power spectral density of $r_I(t)$ and $r_Q(t)$ can be easily calculated by taking

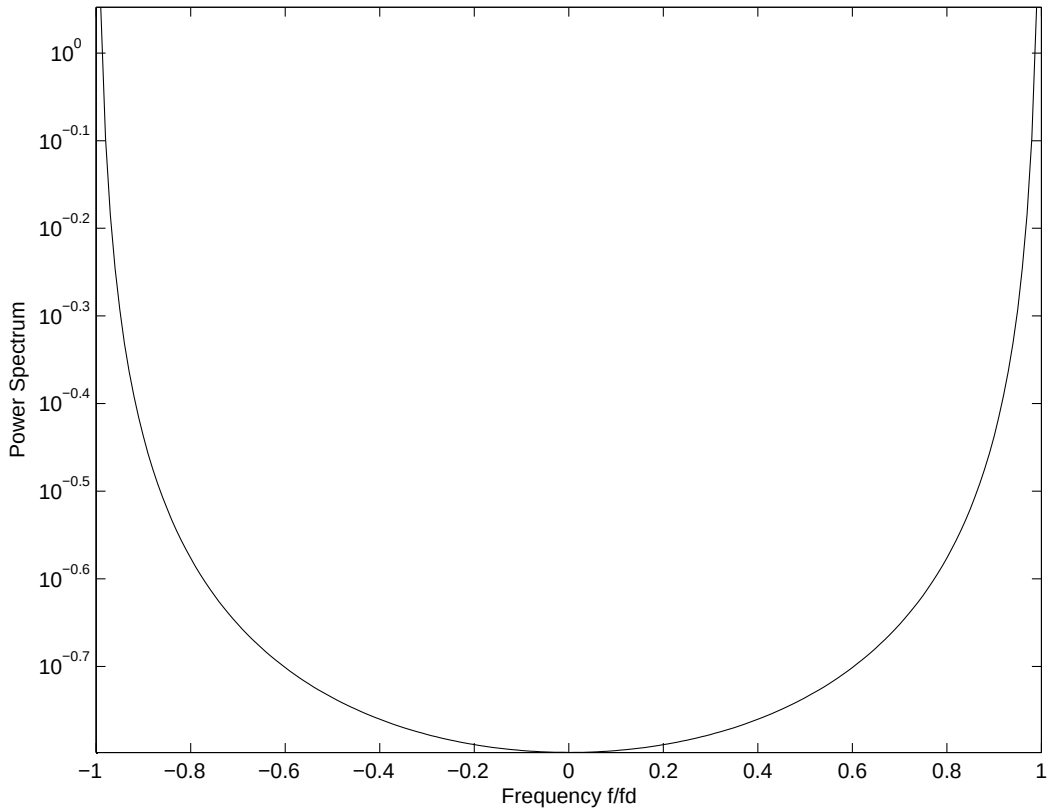


Fig. 5. Power spectrum of Rayleigh fading process

the Fourier transform of $\phi_{r_I r_I}(\tau)$,

$$S_{r_I r_I}(f) = \begin{cases} \frac{1}{2\pi f_d} \frac{1}{\sqrt{1-(f/f_d)^2}} & |f| \leq f_d \\ 0 & otherwise. \end{cases} \tag{2.18}$$

The bathtub shape of the spectrum is shown in Figure 5.

### 2. Level crossing rate and fade duration

Two important second order statistics associated with Rayleigh fading are level crossing rate and fade duration. The level crossing rate of Rayleigh fading envelope $L_R$, is defined as the rate at which the envelope crosses the level R in the positive (or

negative) going direction. It is given by the formula [12]

$$L_R = \sqrt{2\pi} f_d \rho e^{\rho^2}, \tag{2.19}$$

where $\rho = R/R_{RMS}$.

The average fade duration $\bar{\tau}$ is defined as the average period of time for which the received signal remains below a specified level R. Consider a very long time interval T in which $t_i$ denotes the duration of the ith fade below the level R. The probability of the fading envelope level being less that R is

$$Pr[r < R] = \frac{1}{T} \sum_i t_i. \tag{2.20}$$

From the above equation, fade duration can be derived as

$$\bar{\tau} = \frac{1}{T L_R} \sum_i t_i = \frac{Pr[z \leq R]}{L_R}. \tag{2.21}$$

For Rayleigh distribution,

$$Pr[r \leq R] = \int_0^R p(r) dr = 1 - e^{-\rho^2} \tag{2.22}$$

and that results in the formula,

$$\bar{\tau} = \frac{e^{\rho^2} - 1}{\sqrt{2\pi} \rho f_d}. \tag{2.23}$$

It has not been very clearly demonstrated how each of these properties affect the results of the simulations of wireless communication systems. Different simulation techniques for the Rayleigh fading channel produce processes that have properties that agree with the above properties with varying degrees of accuracy.

# CHAPTER III

## RAYLEIGH FADING PROCESS GENERATION METHODS

### A. Sum of sinusoids or Jakes method

This popular method for generating a Rayleigh fading process is based on the underlying physical mechanism which causes fading. This method assumes a macrocell kind of a scenario where the basestation is taller than the scatterers and most of the scatterers are located near the mobile receiver. The scatterers are evenly placed on a circular ring about the mobile as shown in Figure 6. This method assumes stationarity and equal strength multipath components ($\alpha_n = 1$). The multipath components arriving at the MS antenna have random phases $\theta_n$, which have uniform distribution in the interval $[0, 2\pi]$ and the angle of arrival is uniformly spaced between $-\pi$ and $\pi$. If the total number of sinusoids is N, the Rayleigh fading process is given by,

$$r(t) = \sqrt{\frac{2}{N}} \sum_{n=1}^{N} e^{-j(2\pi \cos(2\pi \frac{n}{N})t + \theta_n)}. \tag{3.1}$$

By the central limit theorem, as the number of sinusoids becomes large the sum approaches a complex Gaussian random process with the required properties of the Rayleigh fading process. This method, though having the capability of generating variates whose characteristics closely follow those of Rayleigh fading process, requires a large number of sinusoids and hence is cumbersome to use in simulations.

A modified sum of sinusoid method of generation of Rayleigh distributed variates is explained in [12]. The total number of oscillators N, is always of the form 4M+2. In this case, the received complex low-pass envelope is given by

$$r(t) = \sum_{n=1}^{N} e^{-j(\hat{\phi}_n + 2\pi f_d t \cos\theta_n)}, \tag{3.2}$$

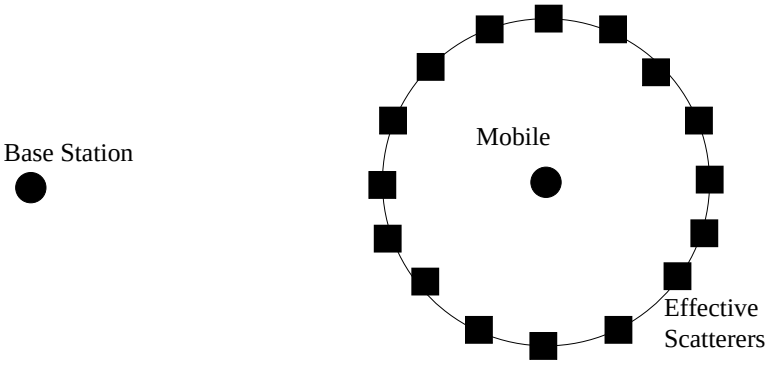


Fig. 6. Jakes' model

where $\hat{\phi}_n = 2\pi(f_c + f_d)\tau_n$. The angles of arrival of the multipath components $\theta_n$ are given by

$$\theta_n = \frac{2\pi n}{N}. \tag{3.3}$$

Since N/2 is odd, 3.2 can be modified as follows:

$$\begin{aligned} r(t) &= \sum_{n=1}^{N/2-1} [e^{-j(\hat{\phi}_{-n}+2\pi f_d t\cos\theta_n)} + e^{-j(\hat{\phi}_n+2\pi f_d t\cos\theta_n)}] \\ &\quad + e^{-j(\hat{\phi}_{-N}+2\pi f_d t)} + e^{-j(\hat{\phi}_N+2\pi f_d t)} \\ &= \sqrt{2}\sum_{n=1}^{M}[e^{-j(\hat{\phi}_{-n}+2\pi f_d t\cos\theta_n)} + e^{-j(\hat{\phi}_n+2\pi f_d t\cos\theta_n)}] \\ &\quad + e^{-j(\hat{\phi}_{-N}+2\pi f_d t)} + e^{-j(\hat{\phi}_N+2\pi f_d t)}. \end{aligned} \tag{3.4}$$

The simplification in equation 3.4 is possible because in the first summation, the frequencies from $-2\pi f_d \cos(2\pi/N)$ to $2\pi f_d \cos(2\pi/N)$ are used twice and in the second summation they are used only once to reduce complexity. The equation can be further simplified using trigonometric identities to get

$$r(t) = \sqrt{2}\{[2\sum_{n=1}^{M}\cos\beta_n \cos 2\pi f_n t + \sqrt{2}\cos\alpha\cos 2\pi f_d t]$$

$$+j[2\sum_{n=1}^{M}\sin\beta_n\cos 2\pi f_n t+\sqrt{2}\sin\alpha\cos 2\pi f_d t]\}$$
$$= \sqrt{2}[2\sum_{n=1}^{M}e^{j\beta_n}\cos 2\pi f_n t+\sqrt{2}e^{j\alpha}\cos 2\pi f_d t], \quad (3.5)$$

where $f_n = f_d\cos(2\pi n/N)$, $\alpha$ is an arbitrary phase and $\beta$ is a gain. The parameters $\alpha$ and $\beta_n$ can be chosen such that $< r_I^2(t) >=< r_Q^2(t) >$ and $< r_I(t)r_Q(t) >= 0$, where $< . >$ is a time average operator. These conditions are satisfied by choosing $\alpha = 0$ and $\beta_n = \pi n/M$.

This method will hence forth be referred to as Jakes2 in this report. If the first Jakes method utilizes N oscillators to simulate a particular number of incoming waves, the Jakes2 method uses $\frac{1}{2}(\frac{N}{2}-1)$ oscillators. It can be seen that there are no random variables involved in the Jakes2 method. So, when using this method to generate Rayleigh fading processes, each and every process will be the same. To generate two different processes, r(t) can be used from two different time intervals from t1 to t2 and from t3 to t4 such that the two intervals do not overlap.

## B. IDFT method

This method generates Rayleigh distributed variates with the required ACF properties. In this method, complex zero-mean Gaussian noise (A(k)+jB(k)) is first generated, with the real and complex parts independent and identically distributed (i.i.d). This complex vector is multiplied with a real valued vector which is equivalent to a vector with filter coefficients (F(k)).

$$R(k) = F(k)(A(k) + jB(k)). \quad (3.6)$$

Then, the IDFT of the resultant vector gives the required process r(n), n=0,1,...,N-1.

$$r(n) = \frac{1}{N} \sum_{k=0}^{N-1} F(k)(A(k) + jB(k))e^{j(2\pi kn/N)}. \tag{3.7}$$

The method was first proposed in [11] and later developed in [14] and [13]. The values of the filter coefficients F(k) will decide the properties of the generated process. If the required ACF can be defined as follows:

$$\phi_{r_I r_I}[d] = \phi_{r_Q r_Q}[d] = \phi_R[d] \tag{3.8}$$

$$\phi_{r_I r_Q}[d] = \phi_{r_Q r_I}[d] = \phi_I[d] \tag{3.9}$$

$$\phi = \phi_R + j\phi_I, \tag{3.10}$$

then it is shown in [14] that the filter coefficients can be calculated as

$$\phi[d] \overset{DFT}{\leftrightarrow} (F[k])^2, \tag{3.11}$$

where $(F[k])^2$ is a positive real sequence. But for Rayleigh fading $\phi$ is a real vector making $(F[k])^2$ a complex number. So, F[k] can be approximated as

$$F_S[k] = \sqrt{S_{r_I r_I}\left(\frac{kf_s}{N}\right)}. \tag{3.12}$$

This approximation causes $\phi_I$ to be non zero. This problem can be averted.

Let $\Phi_{CS}$ and $\Phi_{CAS}$ be two sequences defined as

$$\phi_R[d] \overset{DFT}{\leftrightarrow} \Phi_{CS}[k] \tag{3.13}$$

$$j\phi_I[d] \overset{DFT}{\leftrightarrow} \Phi_{CAS}[k]. \tag{3.14}$$

This would mean that $\Phi_{CS}$ is a Conjugate-symmetric sequence ($\Phi_{CS}[k] = \Phi^*_{CS}[k]$) and $\Phi_{CAS}$ is a Conjugate-antisymmetric sequence ($\Phi_{CAS}[k] = -\Phi^*_{CAS}[k]$). Due to the

linearity property of DFT,

$$\begin{aligned}\phi[d] &= \phi_R[d] + j\phi_I[d] = IDFT(\Phi[k]) \\ &= IDFT(\Phi_{CS}[k]) + IDFT(\Phi_{CAS}[k]).\end{aligned} \tag{3.15}$$

Also note that

$$\Phi_{CS}[k] = \frac{1}{2}\Phi[k] + \frac{1}{2}\Phi^*[N-k] \tag{3.16}$$

$$\Phi_{CAS}[k] = \frac{1}{2}\Phi[k] - \frac{1}{2}\Phi^*[N-k]. \tag{3.17}$$

To get $\phi_I = 0$, it is required to make $\Phi_{CAS} = 0$. This can be done by using equation 3.16 to define a new set of filter coefficients

$$F_M(k) = \begin{cases} F_S[k], & k = 0 \\ \frac{1}{\sqrt{2}}F_S[k], & k = 1, 2, ..., \frac{N}{2} - 1 \\ F_S[k], & k = \frac{N}{2} \\ \frac{1}{\sqrt{2}}F_S[k], & k = \frac{N}{2} + 1, ..., N - 1. \end{cases} \tag{3.18}$$

But this $F_M(k)$ cannot be directly used in a generator. Some minor changes have to be made to improve the performance. The desired output of the generator is Rayleigh distributed. This means that the real and imaginary components should have zero mean. For N finite and F[0] non zero, that is not possible with this method. The mean of the r[n] generated will be R[0]=F[0]A[0]+jF[0]B[0]. The process thus generated will have a non zero mean and hence will have a Ricean distribution. To force the mean to be zero, R[0] should be forced to zero which can be accomplished by having F[0] as zero. In this case, the mean of the process will be identically zero for every realization.

The exact realization of the ACF and the bandlimited power spectrum is not possible with this algorithm. Due to the truncation of the time sequence, Gibbs

oscillations occur at the points of discontinuities in the frequency domain. Since the power spectrum is forced to be band limited, there will be aliasing in time domain. The initial approach of defining the filter coefficients by sampling the continuous-time power spectrum (equation 3.12) effectively ignores the finite-time effects. This problem can be removed by changing the filter coefficients at the point at index $k_m$ which is at, or just below, the maximum Doppler frequency ($k_m = \lfloor N f_m \rfloor$). The filter coefficient of $k_m$ is chosen such that the area under an interpolation of the spectrum coefficients is the same as the area under the continuous-time spectrum curve. The realized maximum Doppler frequency in the generated process is $k_m f_s/N$. The area under the power spectrum curve with the modified Doppler frequency, from zero to analog frequency f is given in [14] as

$$C(f) = \frac{k_m f_s}{N} \arcsin\left(\frac{fN}{f_s k_m}\right), 0 \leq f \leq \frac{k_m f_s}{N}. \tag{3.19}$$

The area under the portion of the power spectrum between the frequencies $(k_m - 1)f_s/N$ and $k_m f_s/N$ is equal to $C(k_m f_s/N) - C([k_m - 1]f_s/N)$. Equating this area to the rectagular area of height $(F[k_m])^2$ and width $f_s/N$,

$$F[k_m] = \sqrt{k_m \left[\frac{\pi}{2} - \arctan\left(\frac{k_m - 1}{\sqrt{2k_m - 1}}\right)\right]}. \tag{3.20}$$

The final filter coefficients F(k) is determined using equations 3.12, 3.18, and 3.20. For the required Rayleigh distributed process, the filter sequence is given by

[14]

$$F(k) = \begin{cases} 0, & k = 0 \\ \sqrt{\frac{1}{2\sqrt{1-(\frac{k}{Nf_m})^2}}}, & k = 1, 2, ..., k_m - 1 \\ \sqrt{\frac{k_m}{2}[\frac{\pi}{2} - arctan(\frac{k_m - 1}{\sqrt{2k_m - 1}})]}, & k = k_m \\ 0, & k = k_m + 1, ...N - k_m - 1 \\ \sqrt{\frac{k_m}{2}[\frac{\pi}{2} - arctan(\frac{k_m - 1}{\sqrt{2k_m - 1}})]}, & k = N - k_m \\ \sqrt{\frac{1}{2\sqrt{1-(\frac{N-k}{Nf_m})^2}}}, & k = N - k_m + 1, ..., N - 2, N - 1. \end{cases} \tag{3.21}$$

IDFT is a linear process. So, if the input is complex Gaussian noise, the final process' real and imaginary parts are also Gaussian distributed. If N is a power of 2, IFFT can be applied for IDFT making the whole process very efficient. Due to this reason, even if N is not a power of 2, $2^{(\lceil \log_2 N \rceil)}$ variates are generated and the first N points are chosen.

## C. Filtering white Gaussian noise

The third method of generating the Rayleigh fading process is by filtering complex white Gaussian noise. Since the filtering operation is linear, the output of the filter is also Gaussian distributed, but colored [5]. The magnitude of the output will be Rayleigh distributed. The major limitation of this method is that it can produce only rational forms of power spectra. Of the three methods discussed till now, this one is the most flexible in the sense that the type and the order of the filter can be changed according to the result that is required. The filter can be designed to approximate a desired power spectral density or the autocorrelation function.

IIR low-pass filters can used to approximate the required spectral characteristics. A first order filter would provide an autocorrelation function that is totally off the

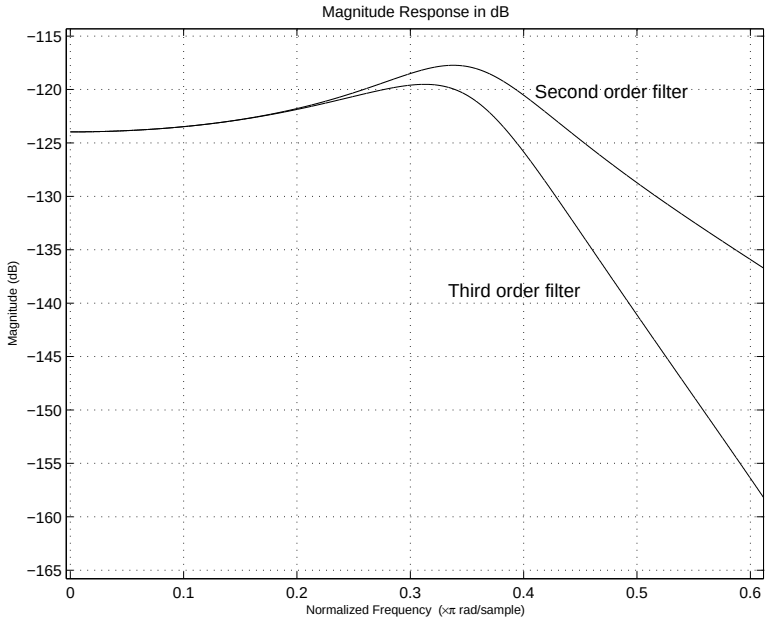


Fig. 7. Magnitude response of second and third order filters

mark and a level crossing rate that is approximately five times the required value. A second order filter gives an autocorrelation function that closely follows the bessel function until the first minima but again the level crossing rate values are 15% higher than the required value. The second order filter is a lowpass filter given by [10]

$$H(s) = \frac{\omega_0^2}{s^2 + 2\xi\omega_0 s + \omega_0^2}. \tag{3.22}$$

As it can be seen from Figure 7 that the magnitude response of the second order filter is high for higher frequencies. To improve the performance, this filter can be cascaded with a lowpass filter to filter out high frequency components. It was found that third order lowpass filters (second order filter cascaded with a first order lowpass filter) provide a good approximation to the required autocorrelation characteristics and level crossing rates. As shown in Figure 8, higher order filters do not provide the

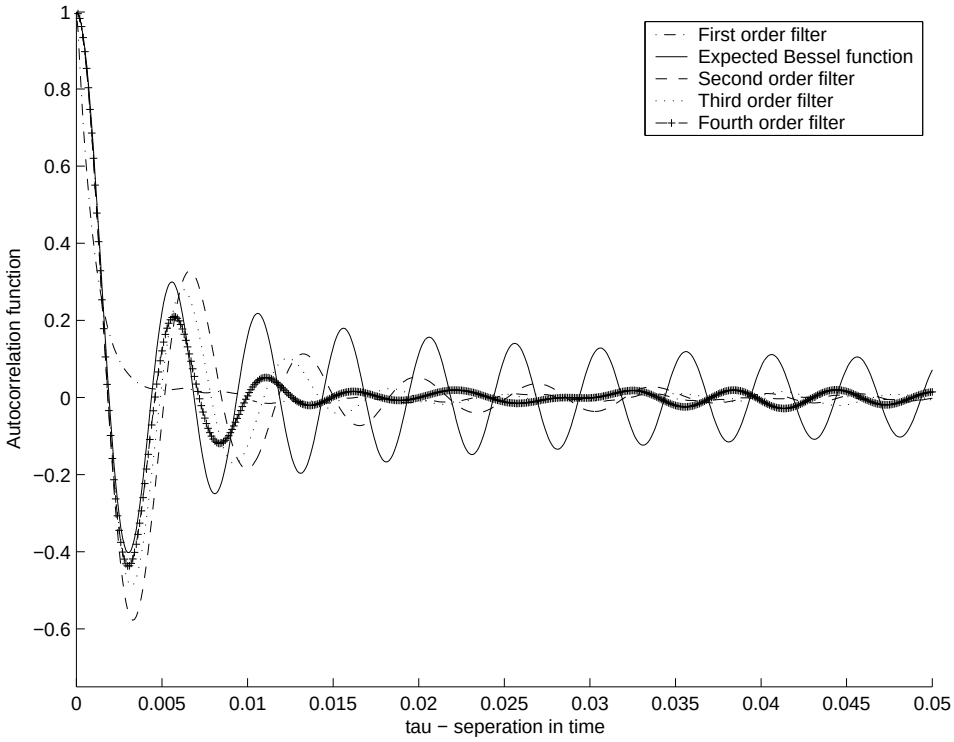


Fig. 8. The autocorrelation function produced by filters of different orders

justification for the increase in the complexity and lower order filters provide a poor and ACF and level crossing rate approximation.

The third order filter is described as follows

$$H(s) = \frac{\omega_0^3}{(s+\omega_0)(s^2+2\xi\omega_0 s+\omega_0^2)}. \tag{3.23}$$

This analog filter, then has to be mapped to a digital filter using bilinear transformation.

$$H(z) = H(s)\Big|_{s=2f_s\left(\frac{1-z^{-1}}{1+z^{-1}}\right)}, \tag{3.24}$$

where $\omega_0 = 2\pi f_d/1.2$ and $\xi = 0.175$. These values for $\omega_0$ and $\xi$ were obtained to

provide the closest visual approximation to the first lobe of the required autocorrelation function. The reason why the autocorrelation property was chosen instead of the spectral characteristic will be explained later.

Rayleigh fading process may also be obtained by passing the complex Gaussian noise through an Autoregressive(AR) filter. Autoregressive Moving Average (ARMA) models are commonly used to simulate many discrete time random processes [4]. AR filters (discrete filters with coefficients only in the denominator) of order n can be designed to produce any autocorrelation function up to n points.

The relationship between the autocorrelation function ($r_{xx}(m)$) and the ARMA(p,q) parameters is given by [7]

$$r_{xx}(m) = \begin{cases} -\sum_{k=1}^{p} a_k r_{xx}(m-k) & m > q \\ -\sum_{k=1}^{p} a_k r_{xx}(m-k) + \sigma_w^2 \sum_{k=0}^{r-m} h(k) b_{k+m} & 0 \leq m \leq q \\ r_{xx}^*(-m) & m < 0 \end{cases} . \tag{3.25}$$

where p denotes the order of the denominator, q denotes the order of the numerator and $\sigma_w^2$ denotes the variance of the white Gaussian noise inout to the filter. For a pure AR process the same equation reduces to

$$r_{xx}(m) = \begin{cases} -\sum_{k=1}^{p} a_k r_{xx}(m-k) & m > 0 \\ -\sum_{k=1}^{p} a_k r_{xx}(m-k) + \sigma_w^2 & m = 0 \\ r_{xx}^*(-m) & m < 0 \end{cases} . \tag{3.26}$$

Equation 3.26 can be solved using Yule-Walker equations to yield the AR filter coefficients as shown below.

$$\mathbf{Ra} = -\mathbf{r}, \tag{3.27}$$

where

$$\mathbf{R} = \begin{bmatrix} r_{xx}(0) & r_{xx}(-1) & . & . & . & r_{xx}(-p+1) \\ r_{xx}(-1) & r_{xx}(0) & . & . & . & r_{xx}(-p+2) \\ \vdots & \vdots & & & & \vdots \\ r_{xx}(p-1) & r_{xx}(p-2) & . & . & . & r_{xx}(0) \end{bmatrix},$$

$\mathbf{a} = [a_1 a_2 ... a_p]^T$ and $\mathbf{r} = [r_{xx}(1) r_{xx}(2) ... r_{xx}(p)]^T$.

For higher order AR models, the above equation tends to have the poles outside the unit circle, making the filter unstable. This problem can be alleviated by using diagonal loading, where a modified autocorrelation matrix $\tilde{\mathbf{R}}$ is used,

$$\tilde{\mathbf{R}}\mathbf{a} = -\mathbf{r}, \tag{3.28}$$

with $\tilde{\mathbf{R}} = \mathbf{R} + \gamma I$. Here, $\gamma$ is a suitable loading parameter ensuring the stability of the filter. $\gamma$ is chosen such that it is the least value that makes the filter stable.

If the autocorrelation has to be matched up to M points, an AR filter of order p=M has to be chosen. If p is high this would increase the complexity of the filter and the loading factor $\gamma$. The solution to this problem is to use a subsampled AR filter to filter the Gaussian noise and pass the output through a multistage interpolator. The AR filter has to be designed using the subsampled autocorrelation

$$r'_{xx}(n) \triangleq r_{xx}(nL), \tag{3.29}$$

where L is the subsampling factor. The order of the filter p, is chosen for this ACF. The interpolation after the initial AR filtering can be achieved by inserting L-1 zeros between every successive point and then passing it through a suitably designed Butter worth filter [9]. The Butterworth filter should have a cut off frequency $\omega_c = \pi/L$. To reduce the complexity, a filter bank can be used instead of the Butterworth filter.

Since these lowpass filters after the interpolation are not ideal, the auto correlation of the process will be slightly altered during this filtering process. It was found that subsampling factors up to 100 did not alter the autocorrelation in any significant amount. But attempts with subsampling factors around 1000 yielded very poor auto-correlation characteristics. So, it is advisable to keep the subsampling factor within 100.

If the point M, up to which the ACF of the process has to closely follow the Bessel function, is too large, the order of the filter to be used is very high even after using subsampled filters. This creates a very complex filter. To counter this problem, a lower order filter can be designed using the least squares modified Yule Walker equation (LSMYWE) method of AR estimation [2], though at the cost of destroying the exact correlation-matching property of AR modeling. LSMYWE method also involves solving the equation 3.27. But now,

$$\mathbf{R} = \begin{bmatrix} r_{xx}(0) & r_{xx}(-1) & . \ . \ . & r_{xx}(-p+1) \\ r_{xx}(-1) & r_{xx}(0) & . \ . \ . & r_{xx}(-p+2) \\ \vdots & \vdots & & \vdots \\ r_{xx}(M-1) & r_{xx}(M-2) & . \ . \ . & r_{xx}(M-p) \end{bmatrix},$$

$\mathbf{a} = [a_1 a_2 ... a_p]^T$ and $\mathbf{r} = [r_{xx}(1) r_{xx}(2) ... r_{xx}(M)]^T$. Here, $M > p$. And $\mathbf{a}$ can be calculated as

$$\mathbf{a} = -(\mathbf{R}^H \mathbf{R})^{-1} \mathbf{R}^H \mathbf{r}. \tag{3.30}$$

The LSMYWE method produces a pth order filter which can output a process whose ACF is the closest to first M points of the Bessel function in the mean square sense.

# CHAPTER IV

## COMPARISON OF RAYLEIGH FADING PROCESS GENERATORS

Three different techniques for generating Rayleigh fading processes were discussed in the previous chapter. Two of these methods can produce the ideal Rayleigh fading process if infinite computing complexity is available. The sum of sinusoids method with infinite number of oscillators or the filtering of Gaussian noise with infinite order AR filter will produce the ideal output required. But in reality, due to the availability of finite computing complexity, the output of the generators are approximating the ideal Rayleigh characteristics. The accuracy of the IDFT method has not yet been discussed in relation to all the characteristics of the Rayleigh fading channel.

While simulating a communication system, it has to be decided as to which generating technique is best suited, so that the results are reliable. While there are a number of quality measures available in literature to compare the generating methods, like weighted mean square error in autocorrelation function, first-order empirical cumulative distribution functions, there is no convincing argument as to why these measures are important in simulating any communication system and how it will affect the output of the simulation. Moreover, there are no specific methods to find out the best generating method for a particular communication system that has to be simulated. This chapter compares the generating techniques in all the Rayleigh Characteristics and finally arrive at the exact quality measures that affect the simulation output of a communication system.

## A. Comparison of characteristics of the generated processes

### 1. Rayleigh distribution

The first characteristic that is expected and is surely required from a Rayleigh fading process generator is that the output is a Rayleigh distributed random variate. This characteristic can be tested by simulating a baseband coherent BPSK modulated communication system over the Rayleigh fading channel simulated by the generators with additive white Gaussian noise (AWGN). The expression for the bit error rate of a BPSK is given by

$$P_{e,BPSK}(\lambda_b) = Q(\sqrt{2\lambda_b}), \tag{4.1}$$

where $\lambda_b = r^2 * SNR$. The above equation gives the conditional error probability with r fixed. To find the expression in which r is random, $P(\lambda_b)$ should be averaged over the probability density function of $\lambda_b$.

$$P_{e,BPSK} = \int P_{e,BPSK}(\lambda_b) p(\lambda_b) d\lambda_b, \tag{4.2}$$

where $p(\lambda_b)$ is the probability density function of $\lambda_b$ when r is random. Since r is Rayleigh distributed, $r^2$ is chi-square distributed. It can be shown that

$$p(\lambda_b) = \frac{1}{\lambda} e^{-\lambda_b/\lambda}, \lambda_b \geq 0, \tag{4.3}$$

where $\lambda$ is the average signal to noise ratio. Substituting equation 4.3 in 4.1 and 4.2, the expected bit error rate (BER) of this communication system can be calculated as shown in [6] as

$$P_{e,BPSK} = \frac{1}{2}(1 - \sqrt{\frac{\lambda}{1+\lambda}}). \tag{4.4}$$

If the generators produce processes that are exactly Rayleigh distributed, the BER of the simulated systems will have the same BER as given by equation 4.4.

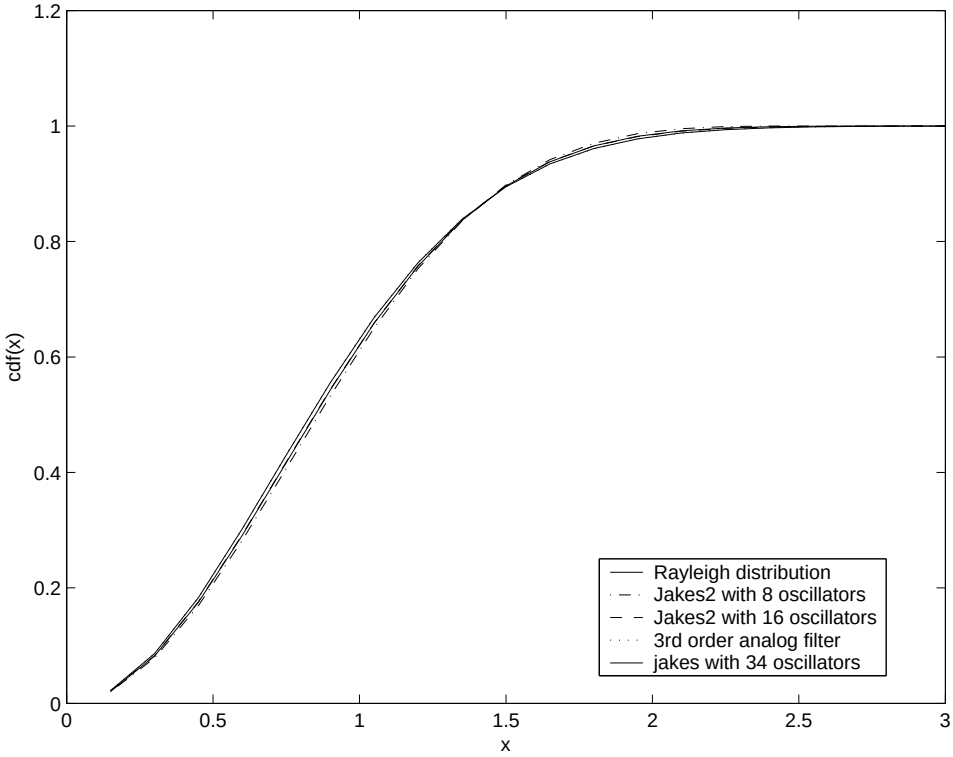


Fig. 9. Cumulative distribution of fading coefficients generated by different methods

The IDFT method and the WGN filtering method are expected to produce Rayleigh distributed output. This is because their generation method involves just linear processing of complex Gaussian noise, which will produce colored, but still Gaussian distributed output, the magnitude of which will have a Rayleigh distribution. Hence simulations having these Rayleigh fading generators will have the expected BER. But the sum of Sinusoid methods will produce Rayleigh fading processes only if infinite number of oscillators are used. This is ilustrated in the Figures 9 and 10.

If a finite number of oscillators are used, the simulations will produce BER curves that are slightly different from the expected curve. The deviation from the expected

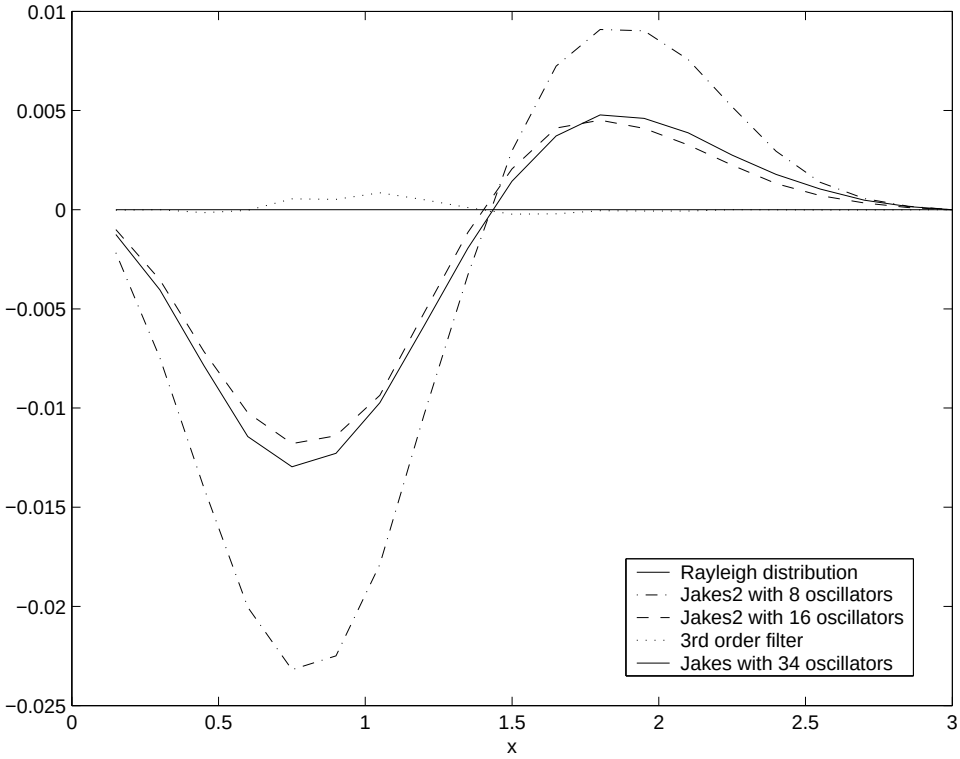


Fig. 10. Difference in cumulative distribution of fading coefficients generated by different methods and the expected Rayleigh distribution

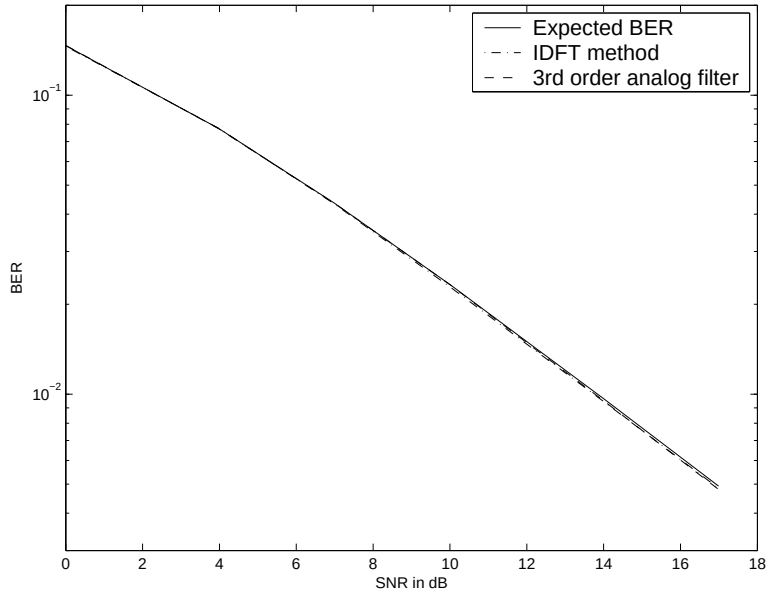


Fig. 11. BER curves for BPSK modulation in Rayleigh fading environment and AWGN using the IDFT method and filtering WGN method

value decreases with the increase in the number of oscillators. The results of the simulation are shown in Figures 11, 12 and 13. It can be seen that as SNR increases, the simulation results from the Jakes methods deviate more from the expected values.

It can be seen that both the Jakes generators produce a BER curve that is lower than the expected value. Similar results can be seen for other modulation techniques like 16-PSK and square 16-QAM. The results of these simulations are shown in Figures 14 and 15.

## 2. Autocorrelation function

The autocorrelation function and the spectrum of the fading process generators are two important and correlated characteristics of the Rayliegh fading process. At present there is no evidence to relate how the difference in the spectrum of the gen-

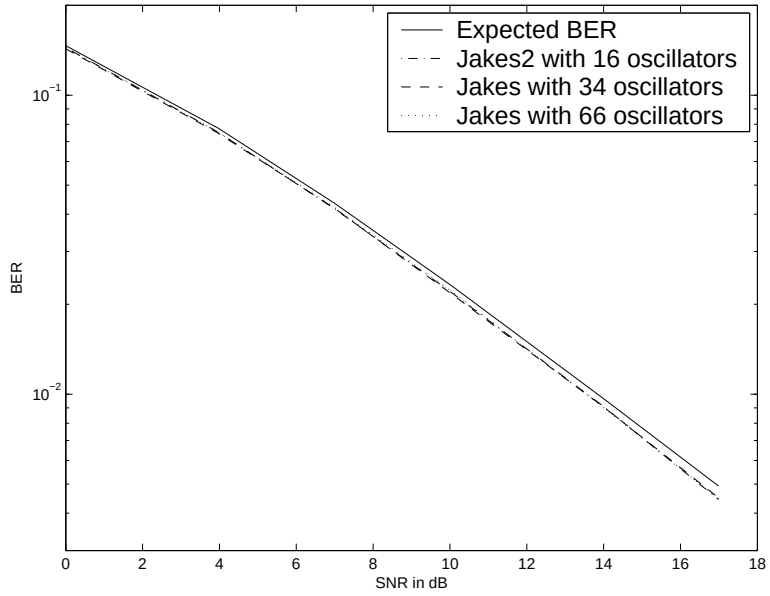


Fig. 12. BER curves for BPSK modulation in Rayleigh fading environment and AWGN using the two Jakes methods

erated process and expected spectrum will affect the result of a simulation. But a difference in the autocorrelation function might affect the simulation results. Before how autocorrelation affects the bit error rate performance is discussed, the concepts of channel coding and interleaving have to be described.

When information is transmitted over a channel in the presence of noise, errors will be introduced. In digital communications, channel coding is a pre-transmission mapping applied to a digital signal, designed to detect or correct these errors. Over a period of years, different kind of channel coding techniques have been introduced to develop more powerful codes that correct more errors with lesser redundancy introduced to the transmitted signal [3]. Block codes (n,k,t) take a block of k bits at a time and code them into n bit blocks. They are capable of correcting up to t bit errors. The factor k/n is a measure of the efficiency of the code. There is no correlation between

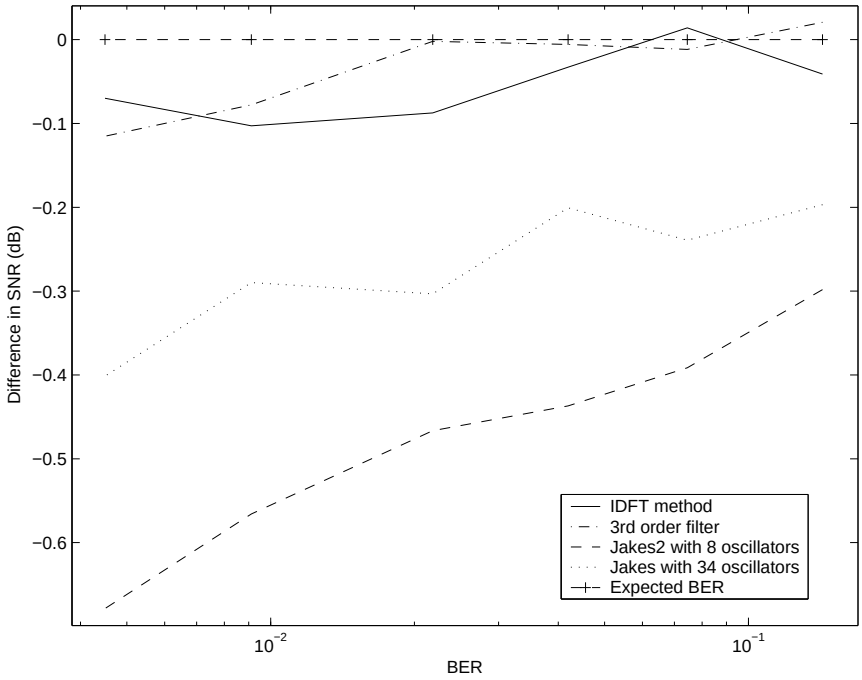


Fig. 13. Difference between simulated BER and expected BER for BPSK modulation in Rayleigh fading environment and AWGN using different Rayleigh fading generators

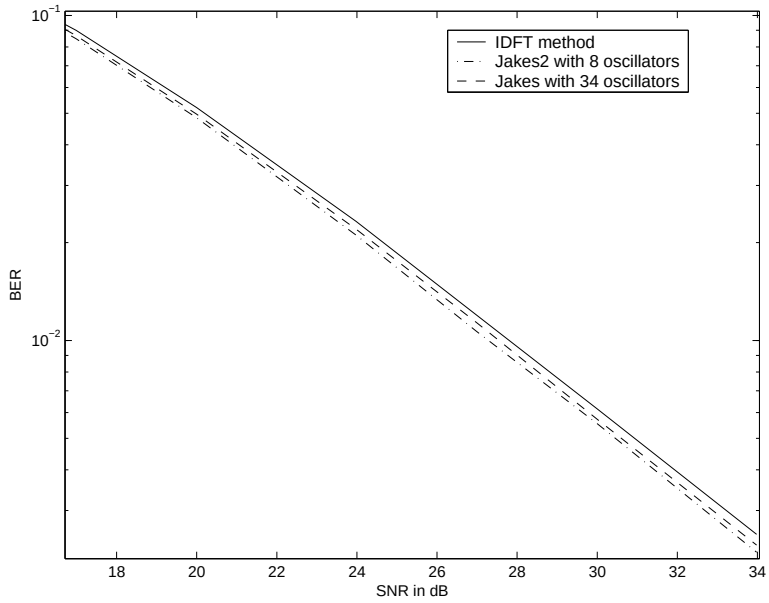


Fig. 14. BER curves for 16-PSK modulation in Rayleigh fading environment and AWGN using different Rayleigh fading generators

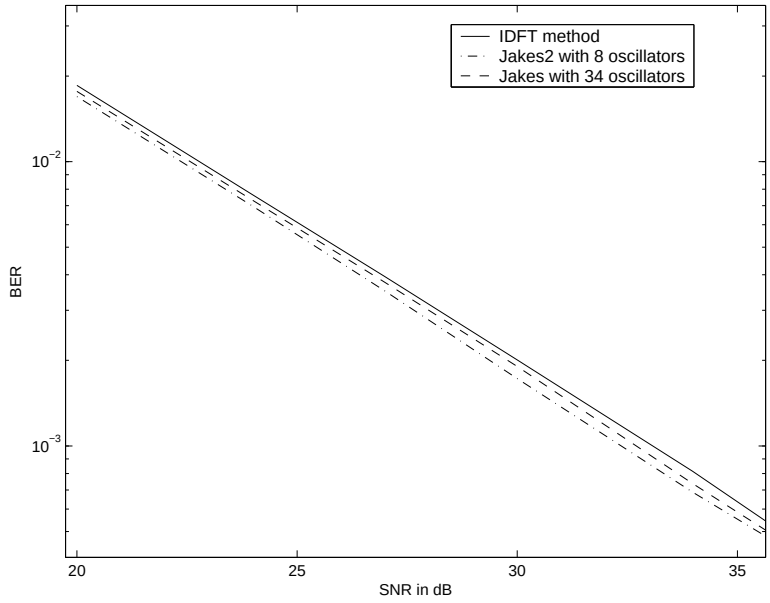


Fig. 15. BER curves for 16-QAM modulation in Rayleigh fading environment and AWGN using different Rayleigh fading generators

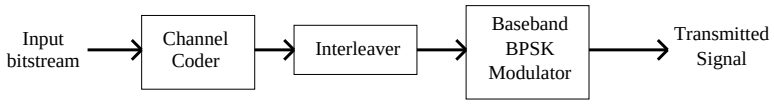


Fig. 16. Block diagram of the simulated transmitter

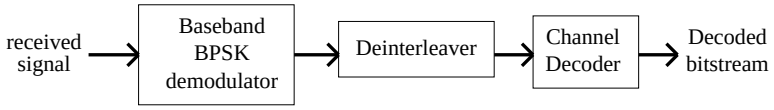


Fig. 17. Block diagram of the simulated receiver

the coding of one block to the next. The BCH code (Bose-Chaudhuri-Hochquenghem code) is a linear cyclic code capable of correcting multiple errors. In BCH codes, n is usually of the form 2m-1. The Golay code (23,12,3) is one other code which can correct upto 3 errors per block. The simulated transmitter is shown in Figure 16.

In wireless fading channels, bit errors occur in bursts. So, the blocks in deep fades have too many errors which overwhelm the error correction capability of the channel codes while blocks where the channel conditions are good hardly have any errors. To spread the errors among the blocks so that the errors can be corrected by the channel decoder, a technique called interleaving is used. In this process, at the transmitter end, bits are filled in a matrix one row at a time and then read column wise. This process makes adjacent bits move far away in time, hence distributing the burst errors among different codes. At the receiver end, the reverse process is followed to retrieve the original bitstream. The size of the interleaving matrix determines how far the adjacent bits are separated in time. The simulated receiver is shown in Figure 17.

If the communication system to be simulated implements a block coding scheme

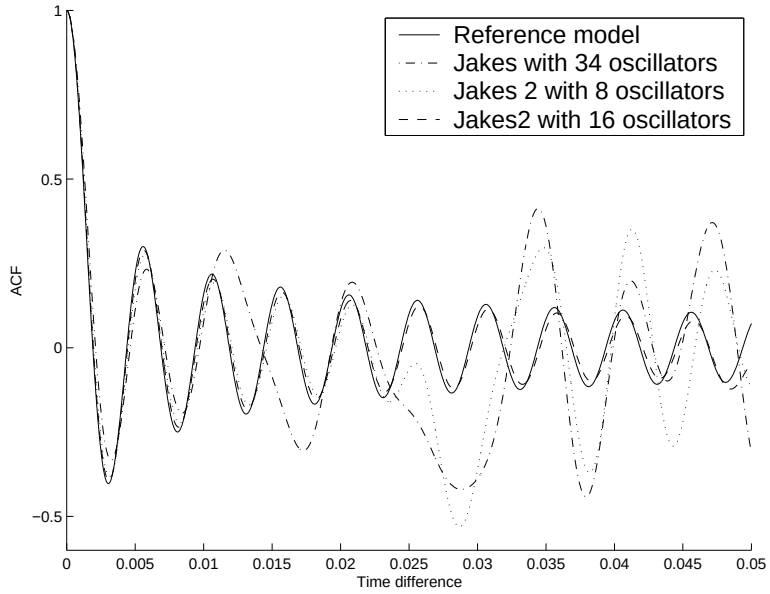


Fig. 18. Autocorrelation of the processes produced by the Jakes methods

with large interleaving blocks, the autocorrelation between the bits in the same coding block affects the result of the simulation. So, it is necessary to make sure that the autocorrelation of the generated process has the exact ACF as the expected one from time difference zero until the maximum time difference between the bits in the same coding block.

The ACF for the fading processes generated by different generators are shown in Figures 18 and 19. The ACF's of the processes generated by the Jakes method follow the Bessel function to a longer time difference if the number of oscillators are increased. In fact, it was found that the time difference up to which the ACF's match was approximately directly proportional to the number of oscillators. The ACF's of the processes generated by the IDFT method, on an average will closely follow the Bessel function. For the filtering of Gaussian noise method, the time difference up to which the ACF follows the Bessel function can be increased by increasing the

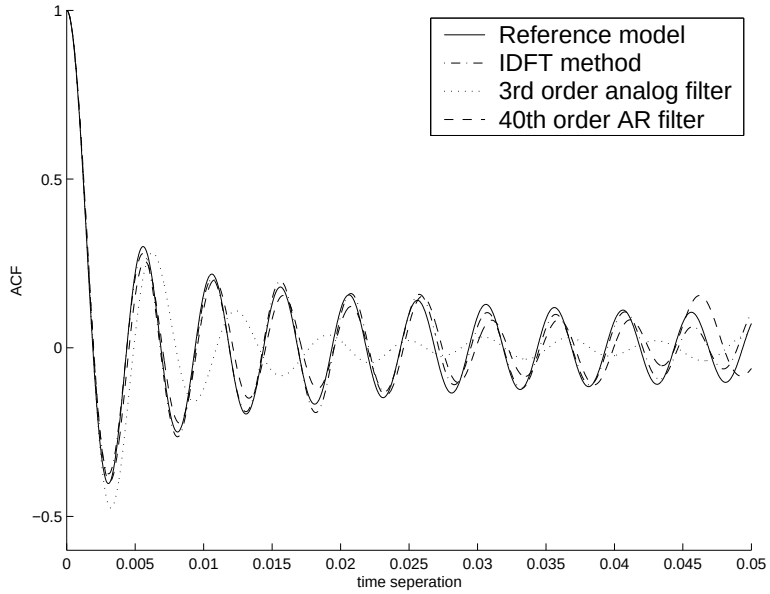


Fig. 19. Autocorrelation of the processes produced by the IDFT method and filtering WGN method

order of the AR filter that is being used by increasing the subsampling factor. Even though both can be increased independently, it should be noted that increasing the subsampling factor beyond 100 will cause the ACF to deviate from the Bessel function. An increase in the order of the analog filter beyond three does not give any substantial improvement in the ACF of the process generated and the small improvement does not justify the increase in complexity.

For example, if a BCH code (127,50,13) is simulated in a Rayleigh fading environment with AWGN along with interleaving block size of 127*4, the maximum time delay between two bits in the same coding block is 508T, where T is the time period of a bit. When simulating this system, the Rayleigh fading process generated should have an ACF that closely follows the Bessel function at least up to 508T to give an accurate result. Baseband simulations were run for this communication sys-

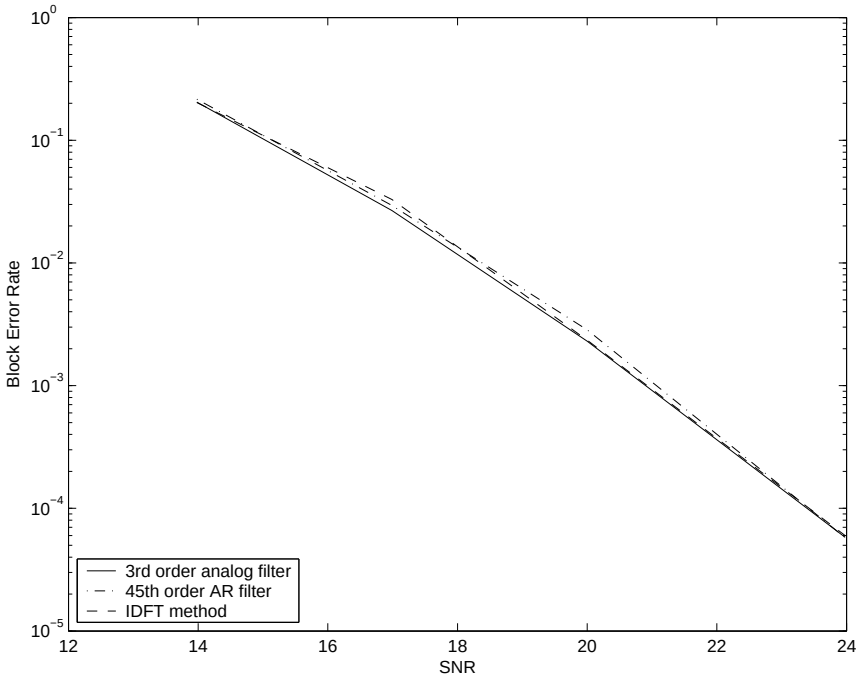


Fig. 20. Simulated block error rates for BCH(127,50,13) code with 127*4 interleaving matrix

tem implementing BPSK modulation with $T = 10^{-4}s$ and sampling frequency for the process $f_s = 10^4/s$ and doppler frequency $f_d = 200Hz$. For the filtering of Gaussian noise method, a 45th order AR filter with a subsampling factor of 9 was used. To simplify the simulation, only block error rate was calculated (a block error for this coding scheme occurs when there are more than 13 errors in a coded block of 127 bits). For this simulation, there are no formulas to give the correct expected results. The results of the simulation are shown in Figure 20.

It can be seen that inspite of the difference in autocorrelation functions in the fading processes generated between the method using the 3rd order filter and the IDFT method, the block error rates simulated are nearly identical. To be sure of this result more simulations were run by reducing the maximum time delay between two

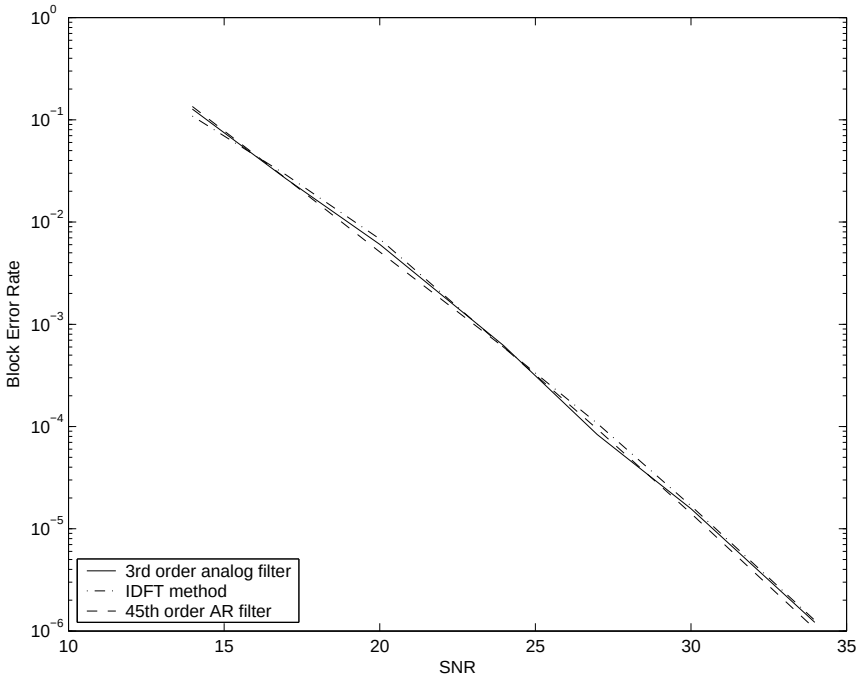


Fig. 21. Simulated block error rates for Golay code with 23*10 interleaving matrix

bits in the same coding block from 508T to 230T (Golay coded system (23,12,3) with 23*10 interleaving matrix size) and 23T (Golay coded system with no interleaving). The results of these simulations are shown in Figures 21 and 22. From these results it can be said that small differences in autocorrelation beyond the first two lobes do not affect the simulation results.

To show that large differences in autocorrelation do make a difference, a simulation was run with Rayleigh fading coefficients generated from a 15th order AR filter, which was designed to produce the autocorrelation shown in Figure 23. The coding scheme used is BCH (127,8,31) code with no interleaving. The difference in results for simulation results using the IDFT method and the filtering of WGN with the 15th order AR filter is shown in Figure 24.

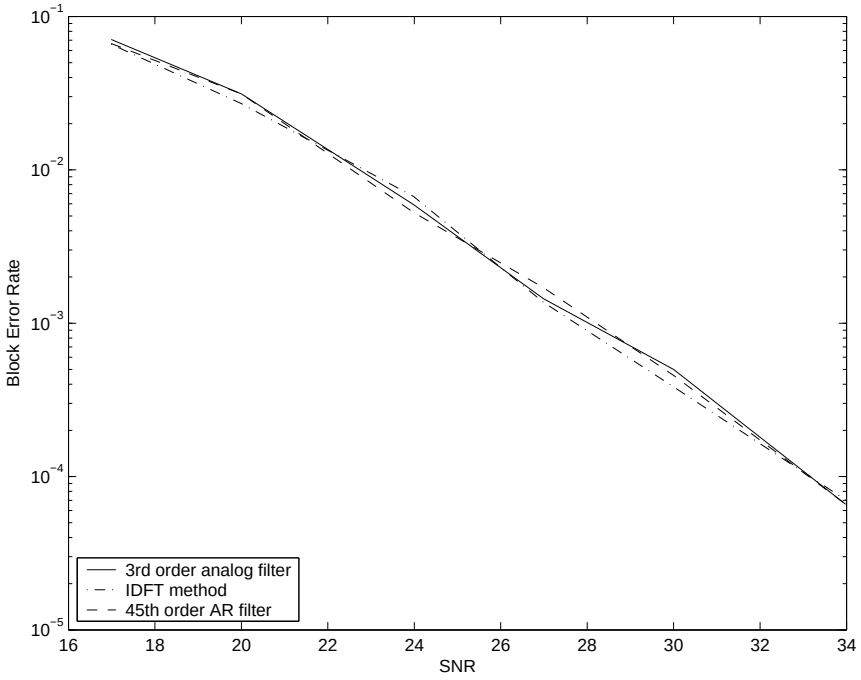


Fig. 22. Simulated block error rates for Golay code

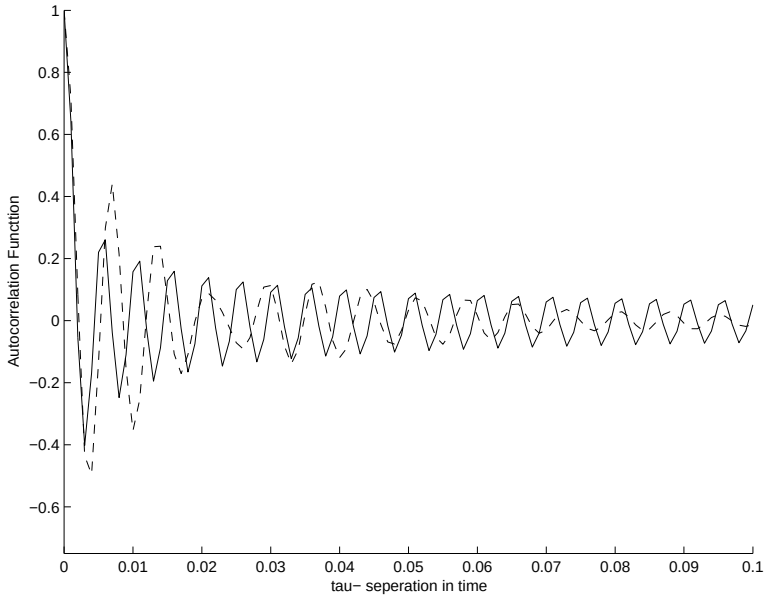


Fig. 23. Autocorrelation function of the Rayleigh fading process generated by the 15th order AR filter

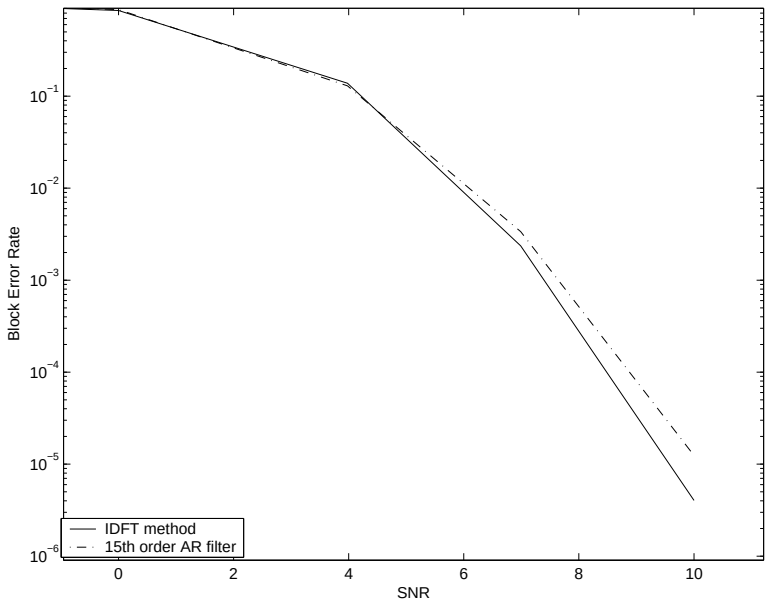


Fig. 24. Simulated block error rates for BCH(127,8,31) code

### 3. Fade duration and level crossing rate

The fade duration and the level crossing rate characteristics of the Rayleigh fading process are interrelated. If a particular generation method does produces a process that has a higher fade duration, that would mean that any simulation of a communication system using this method will yield a result with more number of errors in each burst of bit errors, though the total number of bit errors over a long period of time will be the same if the process is still Rayleigh distributed. Directly opposite will be the effect if the process has a lower fade duration.

To compare these two properties of the processes generated, one thousand processes were independently generated for each technique and the Level crossing rate and the fade duration values were calculated. Each process was 300,000 points long with sampling frequency $3 * 10^4 Hz$ and maximum Doppler frequency of 200Hz. It was noted that at higher values (around 0.1*rms), the processes from all the methods had the expected level crossing rates. But at very low levels (around 0.01*rms), this was not the case. Two set of simulations were run. In the first one, the level crossing rate and fade duration were calculated for a level of 0.3*rms and in the next one, the same were calculated for a level of 0.02*rms. The numbers 0.3 and 0.02 were chosen just to give a perspective of the results. The results are given in Table I. Note that all the values shown in the table are normalized to the expected values.

It can be seen from the results that all the generation methods produce results that closely follow the expected results. The closest results are produced by the filtering WGN method and the IDFT method. The sum of sinusoids methods produce results closer to the expected results as the number of oscillators are increased.

Table I. Level crossing rate and fade duration of the Rayleigh fading processes got from different generators and normalized to the expected values

| Generation method | *level=0.02*rms* | | *level=0.3*rms* | |
|---|---|---|---|---|
| | Level crossing rate | Fade duration | Level crossing rate | Fade duration |
| Jakes | | | | |
| 34 oscillators | 0.8107 | 1.1754 | 0.999 | 0.965 |
| 66 oscillators | 0.8223 | 1.1935 | 0.995 | 0.985 |
| Jakes2 | | | | |
| 8 oscillators | 0.7576 | 1.1980 | 0.921 | 0.991 |
| 16 oscillators | 0.7806 | 1.2061 | 0.958 | 0.996 |
| 32 oscillators | 0.7953 | 1.2265 | 0.971 | 1.008 |
| IDFT method | 0.8343 | 1.1842 | 0.9982 | 1.0009 |
| Filtering WGN | | | | |
| 3rd order analog filter | 0.8299 | 1.1968 | 1.014 | 0.985 |
| 40th order AR filter | 0.8352 | 1.2069 | 0.9996 | 0.9999 |

## 4. Computational complexity

Other than the previously discussed factors, one other important consideration while choosing a generation method is the time taken to generate the process. To generate N Rayleigh faded variates, the Jakes method with $N_s$ oscillators requires $2NN_s$ Trigonometric calculations and $2NN_s$ floating point additions. For the same number of points and oscillators, Jakes2 method requires $2N(N_s + 1)$ trigonometric calculations, 2N floating point multiplications and $2 * NN_s$ floating point additions. It

has to be noted that if the Jakes method uses $N_s$ oscillators, it is equivalent to the Jakes2 method using $\frac{1}{2}(\frac{N_s}{2} - 1)$ oscillators. To generate N variates using the IDFT method, $\frac{N}{2}\log_2 N$ complex multiplications and $N\log_2 N$ complex additions. Due to this $O(N\log_2 N)$ complexity of this method, the number of calculations per sample increases as the N increases. But the inherent efficiency of IFFT method offsets this effect for most practical sequence lengths. For the filtering of WGN method, 2N normally distributed variates have to be generated. It also requires (2N*order of filter) floating point multiplications and (2N*order of filter) floating point additions. If subsampling is used, this number will increase according to the lowpass filter used for the interpolation.

To compare the computational complexity involved in the different fading process generators, Rayleigh fading processes of length 200,000 points were generated using the different methods. The sampling frequency used is $3 * 10^4 Hz$ and the maximum Doppler frequency is 200Hz. The processes were generated in Sun machines with 400 MHz SUNW, UltraSPARC-IIi proccessors and 512 MB RAM memory and Solaris 9 operating system using Matlab and the time for generating each process was noted down. The results are displayed in Table II. It should be noted that these numbers are only indicative and will vary depending on the efficiency of the programs used.

It can be seen that the Jakes methods are the most time consuming methods and the IDFT method and filtering WGN method are pretty quick. Increasing the order of the AR filter beyond 30 makes the filtering WGN method slower than the IDFT method.

Table II. Time required to generate 200,000 points of Rayleigh distributed variables using different generation methods

| Generation method | Generation time |
|---|---|
| Jakes | |
| 34 oscillators | 16.98s |
| 66 oscillators | 37.2s |
| Jakes2 | |
| 8 oscillators | 7.07s |
| 16 oscillators | 14.4s |
| IDFT method | 1.43s |
| Filtering of Gaussian noise | |
| 3rd order analog filter | 1.25s |
| 40th order AR filter with 3*3*3 subsampling factor | 2.24s |

# CHAPTER V

## CONCLUSION

The three types of generators were compared using the characteristics of Rayleigh fading process, distribution, autocorrelation function, fade duration and level crossing rate and computational complexity.

When comparing the different process generators, it was seen that the filtering of WGN method has good Level crossing rate and Fade duration properties. The autocorrelation property of the processes generated by this method can be made to follow the ideal ACF closely until any point we want at the cost of increase in complexity. It has also been shown that the order of the filter can be increased to very high values like 400 with no loss of stability. The computation time for the process generation for the filtering of WGN method is higher only to the IDFT method, and that too only if the order of the filter is greater than 30. One of the disadvantages of the filtering of WGN method is that it requires some time at the start of the simulation to decide the order of the filter and also to design the filter. But this time is spent only once, and the filter thus designed can be used for generating all the processes for simulating a particular communication sytem. But if systems with long blocks of codes require long filters and that increases the complexity of the simulation.

The two Jakes methods discussed have the same advantages in the properties like ACF, Level crossing rate and fade duration. But the problem here is that the process generated by this method will have a perfect Rayleigh distribution only if infinite number of oscillators are used. The computational time to generate a process with this method is the highest of the three methods. The generated process tends to be deterministic and repeat itself after some time.

The IDFT method is one of the fastest methods to generate the Rayleigh fading process and it also has the best autocorrelation property of all the three generators. But this is not necessary for time differences beyond a particular point, which varies with each communication system. Also, the Level crossing rate and the fade duration properties of the processes generated by this method are very close the theoretical values. But the IDFT method requires all the required samples to be generated in one single IDFT operation. This increases the required memory to generate the variates. While interpolation can be used to alleviate this problem in many practical cases, that would mean an increase in the computation time. The advantage of the Sum of Sinusoids methods and the filtering of WGN methods is that, the process samples can be generated as and when required and hence are much less demanding on the memory requirement on the working stations. These methods can be used easily in simulation softwares like simulink which simulate one point at a time.

In summary, from the various measures for comparing of the different Rayleigh fading process generators, it can be said that the choice of Rayleigh fading generators depends on the type of communication system to be simulated. For simulating simple systems like BPSK modulated data with no coding, the magnitude of the complex Gaussian noise is an accurate Rayleigh fading generator. For coded systems, IDFT method and filtering of WGN method are good Rayleigh fading process generators. But the IDFT method is time consuming while simulating long Rayleigh fading processes.

# REFERENCES

[1] W. Jakes, Ed., *Microwave Mobile Communications*, New York: Wiley, 1974.

[2] S.M. Kay, *Modern Spectral Estimation: Theory and Application*, Englewood Cliffs, N.J. : Prentice Hall, 1988.

[3] S. Lin and D.J. Costello, *Error Control Coding: Fundamentals and Applications*, Upper Saddle River, N.J. : Pearson-Prentice Hall, 2nd edition, 2004.

[4] A.V. Oppenheim and R.W. Schafer, *Discrete-time Signal Processing*, Upper Saddle River, N.J. : Prentice Hall, 2nd edition, 1999.

[5] A. Papoulis and S.U. Pillai, *Probability, Random Variables, and Stochastic Processes*, Boston : McGraw-Hill, 4th edition, 2002.

[6] J.G. Proakis, *Digital Communications*, New York: McGraw-Hill, 2nd edition, 1989.

[7] J.G. Proakis and D.G. Manolakis, *Digital Signal Processing: Principles, Algorithms, and Applications*, Upper Saddle River, N.J. : Prentice Hall, 3rd edition, 1996.

[8] T.S. Rappaport, *Wireless Communications: Principles and Practice*, Upper Saddle River, N.J. : Prentice Hall PTR, 2nd edition, 2002.

[9] D. Schafhuber, G. Matz and F. Hlawatsch, "Simulation of wideband mobile radio channels using subsampled ARMA models and multistage interpolation," in *Proceedings of the 11th IEEE Signal Processing Workshop*, IEEE, Singapore, pp. 571-574, August, 2001.

[10] R. Schaumann and M.E.V. Valkenburg, *Design of Analog Filters*, New York: Oxford University Press, 2003.

[11] J.I. Smith, "A computer generated multipath fading simulation for mobile radio," *IEEE Transactions on Vehicular Technology*, vol. VT-24, pp. 39-40, August 1975.

[12] G.L. Stuber, *Principles of Mobile Communication*, Boston: Kluwer Academic, 1996.

[13] D.J. Young and N.C. Beaulieu, "A quantitative evaluation of generation methods for correlated Rayleigh Random variates," in *IEEE Globecom*, Sydney, Australia, Nov. 1998, pp. 3332-3337.

[14] D.J. Young and N.C. Beaulieu, "The generation of correlated Rayleigh random variates by inverse discrete fourier transform," *IEEE transactions on Communications*, vol. 48, pp. 1114-1127, July 2000.

# VITA

Vishnu Raghavan Sathini Ramaswamy was born on March 4th 1982 in Theni, India. He received his B.E.(hons) Electrical and Electronics Engineering from BITS, Pilani, India in 2003. He received a Master of Science degree in Electrical Engineering from Texas A&M University in December 2005.

Vishnu has acquired professional internship experiences with DaimlerChrysler Research Center, Bangalore, India (Jan.-Jun. 2003) and Ericsson, Dallas (May-Aug. 2005). He can be reached by e-mail at vishnu_raghavan@yahoo.com. His permanent mailing address is 6, George Town, Coimbatore-641005, India.

The typist for this thesis was Vishnu Raghavan Sathini Ramaswamy.